

c-Jun N-terminal kinase activation contributes to reduced connexin43 and development of atrial arrhythmias

Jiajie Yan^{1,2,3}, Wei Kong^{2,3}, Qiang Zhang^{1,2,4}, Eric C. Beyer⁵, Gregory Walcott^{1,2}, Vladimir G. Fast^{2,3}, and Xun Ai^{1,2,3,6*}

¹Department of Medicine, University of Alabama at Birmingham, Birmingham, AL, USA; ²Cardiac Rhythm Management Lab UAB, 1670 University Blvd, Volker Hall Rm B149, University of Alabama at Birmingham, Birmingham, AL 35294, USA; ³Department of Biomedical Engineering, University of Alabama at Birmingham, Birmingham, AL, USA; ⁴Division of Internal Medicine, Suzhou Municipal Hospital, Suzhou, China; ⁵Department of Pediatrics, University of Chicago, Chicago, IL, USA; and ⁶UAB Center for Aging, University of Alabama at Birmingham, Birmingham, AL, USA

Received 23 July 2012; revised 18 November 2012; accepted 6 December 2012; online publish-ahead-of-print 14 December 2012

Time for primary review: 42 days

Aims

c-Jun N-terminal kinase (JNK) activation is implicated in cardiovascular diseases and ageing, which are linked to enhanced propensity to atrial fibrillation (AF). However, the contribution of JNK to AF remains unknown. Thus, we assessed the role of JNK in remodelling of gap junction connexin43 (Cx43) and development of AF.

Methods and results

AF induction, optical mapping, and biochemical assays were performed in young and aged New Zealand white rabbit left atria (LA) and cultured HL-1 atrial cells. In aged rabbit LA, pacing-induced atrial arrhythmias were dramatically increased and conduction velocity (CV) was significantly slower compared with young controls. Aged rabbit LA contained 120% more activated JNK and 54% less Cx43 than young LA. Young rabbits treated with JNK activator anisomycin also exhibited increased pacing-induced atrial arrhythmias and reduced Cx43 (by 34%), similar to that found in aged LA. In HL-1 cell cultures, anisomycin treatment for 16 h led to 42% reduction in Cx43, 24% reduction in CV, and an increased incidence of irregular rapid spontaneous activities. These effects were prevented by a specific JNK inhibitor, SP600125. Moreover, a 63% reduction in Cx43 after anisomycin treatment for 24 h led to further slowed CV (by 41%) along with dramatically increased irregular rapid spontaneous activity and highly discontinuous conduction. These JNK-induced functional abnormalities were completely reversed by overexpressed exogenous wild-type Cx43, but not by inactive Cx43.

Conclusion

JNK activation contributes to Cx43 reductions that promote development of AF. Modulation of JNK may be a potential novel therapeutic approach to prevent and treat AF.

Keywords

Atrial fibrillation • JNK • Gap junction • Cell–cell communication

1. Introduction

c-Jun N-terminal kinase (JNK) belongs to the family of mitogen-activated protein kinases (MAPK).¹ JNK is activated by MAP kinase kinases (MKK4 and MKK7) in response to various stimuli including UV irradiation, oxidative stress, and inflammatory cytokines.¹ JNK activation has been linked to a number of pathological conditions including heart failure, strokes, diabetes, cellular ageing, cancers, and chronic inflammatory diseases.^{1–3} Although atrial fibrillation (AF) is the most common cardiac arrhythmia of the elderly and makes a significant

contribution to the mortality and comorbidity of heart failure and diabetes,⁴ the role of JNK in the development of AF remains undetermined to date.

Gap junctions are specialized membrane structures that are composed of subunit protein connexins. The relative amounts and distribution of connexins influence electrical and chemical signal propagation throughout the heart.⁵ Remodelling of atrial gap junctions has been linked to the occurrence and maintenance of AF.^{5–7} Emerging evidence suggests that JNK activation might lead to gap junctional remodelling and slowed ventricular conduction.² In the present study,

* Corresponding author: Tel: +1 205 975 2103; fax: +1 205 975 4720, Email: xai1@luc.edu

we conducted electrophysiological and biochemical experiments in young and aged rabbit hearts to test the hypothesis that JNK activation suppresses the abundance of atrial connexin43 (Cx43) and thereby enhances atrial arrhythmogenicity. Since the functional consequences of JNK activation are cell type dependent,⁸ we also utilized monolayer cultures of atrial HL-1 myocytes. These cultured cells offered several advantages: (i) a confluent monolayer of atrial myocytes minimizes distortions in conduction measurements that arise in the 3D structure of the intact heart; (ii) an atrial myocyte culture line without fibroblasts eliminates the interference of the interstitial matrix present in the intact heart; (iii) a confluent monolayer also facilitates manipulation of connexin expression using *in vitro* gene transfer and assessment of functional consequences using optical mapping. Interventions included pharmacological activation of JNK with anisomycin,^{2,9,10} JNK inhibition with SP600125,¹¹ and *in vitro* Cx43 gene transfer. Our results suggest a pivotal role for JNK activation in AF development via Cx43 suppression.

2. Methods

An expanded Methods section is available as Supplementary material online.

2.1 Animals

This investigation conforms to the *Guide for the Care and Use of Laboratory Animals* (NIH Publication, 8th Edition, 2011) and was approved by the UAB Institutional Animal Care and Use Committee. Young (6 months) and aged (54 months) male New Zealand White rabbits ($n = 24$ each) were used for electrophysiological and biochemical studies as described in the following. Prior to studies, rabbits underwent echocardiographic examination under sedation with ketamine hydrochloride (38–45 mg/kg, im, once or twice during the whole echo procedure). All young and aged rabbits were in sinus rhythm and had normal ventricular and atrial dimensions (Supplementary material online, Table 1) from ECG and 2D-echocardiography assessment as previously described.¹² For *in vivo* electrophysiological studies, rabbits were sedated with ketamine hydrochloride (38–45 mg/kg, im) followed by intubation and mechanical ventilation in a surgical plane of anaesthesia. The anaesthesia status of each animal was maintained by inhalation of 2–4% isoflurane delivered in 100% oxygen for an open-chest AT/AF induction procedure. For *ex vivo* optical mapping and biochemical studies, the rabbit was euthanized by intravenous injection (iv) of one high dose of pentobarbital sodium 50 mg/kg and then the heart was harvested. Body weights, heart weights, and lung weights were obtained. Aged left atrial (LA) tissue exhibited markedly increased levels of protein markers¹³ for ageing p15^{INK} and p19^{ARF} (50 and 215%, respectively vs. young controls, $P < 0.05$; Supplementary material online, Figure S1A and B).

2.2 Atrial arrhythmia induction *in vivo*

LA effective refractory period (AERP) was measured using an S1-S2 pacing protocol and atrial arrhythmias (AT/AF) were induced using burst pacing in open-chest hearts in young rabbits with ($n = 4$) or without ($n = 5$) anisomycin treatment (15 mg/kg, iv, four treatments over 9 days)⁹ and aged rabbits without anisomycin treatment ($n = 6$). The pacing-induced rhythm was defined as AT/AF when the atrial bipolar electrogram showed fast (>8 Hz) and regular or irregular beats that lasted for at least 1 s. If the arrhythmia lasted for >30 s, it was terminated by electrical shock. The duration of AT/AF was analysed as the mean value of all episodes in each rabbit. After the AT/AF induction procedure was completed, tissue was dissected and flash-frozen for the immunoblotting assay.

2.3 Optical mapping in Langendorff-perfused rabbit LA

The LA between the appendage and pulmonary veins of Langendorff-perfused young ($n = 9$) and aged ($n = 10$) rabbit hearts was optically mapped. Voltage-sensitive fluorescent signals (Vm; RH-237 dye) were acquired at a spatial resolution of 1.1 mm and the sampling rate of 1 kHz/channel and analysed as previously described.¹⁴ AERP was measured, and AT/AF was induced as already described. Optical Vm signals were used to analyse action potential duration at 60% of full repolarization (APD₆₀). An upstroke slope was calculated as the maximal dV/dt of AP rise.¹⁵ Conduction velocities (CV) at pacing cycle lengths (CLs) of 250, 200, 150, and 100 ms were calculated via vector field analysis based on methods described by others¹⁵ with modification. Owing to the natural inhomogeneity in atrial conduction caused by irregularities in the structure of the atrial wall, analysing anisotropic conduction is an acknowledged technical challenge.¹⁶ Therefore, heterogeneity of atrial conduction was assessed using maximal differences of activation time from optical mapping data as described by others (Supplementary material online).¹⁶

2.4 Biochemical assays

Immunoblotting was performed as previously described^{12,17} and in the Supplementary material online. Confocal microscopic examination of double label immunofluorescent staining for Cx43/N-cadherin and Cx43/Cx40 was performed as previously described.¹² Junctional Cx43 was quantified using a custom programme by identification of Cx43 fluorescence within intercalated discs based on co-localization with N-cadherin. Masson's trichrome staining was used to detect fibrosis based on the area of blue-stained extracellular collagen,¹⁸ which was quantified using a custom programme.

2.5 Cultured HL-1 atrial cells

The mouse atrial myocyte line (HL-1) was obtained from Dr W. Claycomb (Louisiana State University) and cultured as previously described (see details in Supplementary material online). The content and distribution of expressed connexins and other proteins in HL-1 atrial cells were similar to that in rabbit atrial myocytes (Supplementary material online, Figure S1A and B). Atrial myocytes were treated with 50 ng/mL anisomycin^{9,10} with or without 2 μ mol/L SP600125,¹¹ or a corresponding amount of the DMSO solvent for 16 or 24 h followed by biochemical or optical mapping studies. To manipulate Cx43 levels, anisomycin pre-treated (24 h) cells were infected with adenoviruses encoding either wild-type Cx43 (AdCx43WT) or an inactive Cx43 mutant (dominant negative; AdCx43DN) for 24 h as previously described and in Supplementary material online.¹⁷ AdLacZ-infected and DMSO-treated monolayers were used as negative controls. HL-1 monolayers were mapped at a spatial resolution of 0.055 mm and the sampling rate of 2 kHz/channel using a previously described the mapping system for cell cultures (see details in Supplementary material online).

2.6 Statistical analysis

All data are presented as mean \pm SEM. Differences between multiple groups or any two groups were evaluated using one-way ANOVA with the *post hoc* Tukey test or Student's *t*-test. A *P*-value of <0.05 was considered to be significant.

3. Results

3.1 JNK was activated and Cx43 was reduced in aged rabbit LA

Levels of JNK and related upstream regulatory kinases¹ MKK7 and MKK4 were assessed using immunoblotting. Aged rabbit LA contained

2.2 times as much phosphorylated JNK (activated form) when compared with young LA ($P < 0.05$). In contrast, total JNK1 and JNK2 proteins were unchanged (Figure 1A and D). The increases in activated JNK were accompanied by elevated levels of its activators, phosphorylated MKK7 and MKK4, in aged rabbit LA (increased 51 and 57%, respectively, when compared with young rabbits; Figure 1C and D). In contrast, levels of another stress-activated kinase, p38 (which is not directly involved in the JNK pathway), were not different between aged and young rabbit LA (Figure 1B and D).

We also assessed the relative levels of connexins in these atrial samples, and found a 54% decrease in Cx43 in aged vs. young LA ($P < 0.001$; Figure 2A and C). In contrast, Cx40 was abundant in these samples, but its levels did not differ significantly with age (Figure 2A and C). Cx45 was present at a very low (but constant) level in both young and aged LA (Figure 2A). Immunoblots also showed that levels of the adhesive junction protein, N-cadherin, and the sodium channel protein, SCN5A, were not different in young and aged rabbit LA (Figure 2B and C).

To determine whether changes in Cx43 at specific cellular sites were responsible for the reductions of abundance in aged rabbit LA, we performed double immunofluorescent staining with anti-Cx43 and anti-N-cadherin antibodies to identify Cx43 and intercalated discs in the same LA tissue section. We observed that aged rabbit LA exhibited a 25% reduction in the abundance of junctional Cx43, co-localized with N-cadherin at end-to-end connections between myocytes, when compared with that from young ($P < 0.01$; Figure 2D and E). Moreover, the amount and localization of Cx40 in aged rabbit LA remain unchanged in aged LA (vs. young LA; Supplementary material online, Figure S3). These

immunohistological data are consistent with the results from immunoblotting assessment (Figure 2A).

To define alteration of interstitial collagen in aged rabbit LA, we quantified the area of blue-stained extracellular collagen from microscopic images ($\times 40$ magnification) of Masson's trichrome-stained LA tissue sections. There was no significant difference in the areas of interstitial collagens between aged and young LA (Figure 2F and G). No areas with patchy fibrosis were found in aged LA.

3.2 Both ageing and pharmacological activation of JNK led to atrial arrhythmia development *in vivo*

To test the consequences of JNK activation directly, we treated young rabbits with the JNK activator, anisomycin.^{9,10} Homogenates of LA from anisomycin-treated young rabbits showed a 50% increase in phosphorylated JNK and a 34% reduction in Cx43 when compared with untreated controls ($P < 0.05$ and $P < 0.01$, respectively; Figure 3A); in contrast, Cx40 and SCN5A were unchanged (Figure 3A). The anisomycin-induced JNK activation and Cx43 reduction were comparable with the changes found in aged rabbit LA (Figures 2 and 3A).

Next, we tested whether susceptibility to atrial arrhythmia induction was altered in the aged rabbits or anisomycin-treated young rabbits *in vivo* using burst-pacing in open-chest hearts. We observed a significantly increased inducibility of pacing-induced atrial arrhythmias (AT/AF) in both aged rabbits (5/6) and anisomycin-treated young rabbits (4/4), whereas no atrial arrhythmias were induced in any young control rabbits (0/5). The average length of pacing-induced

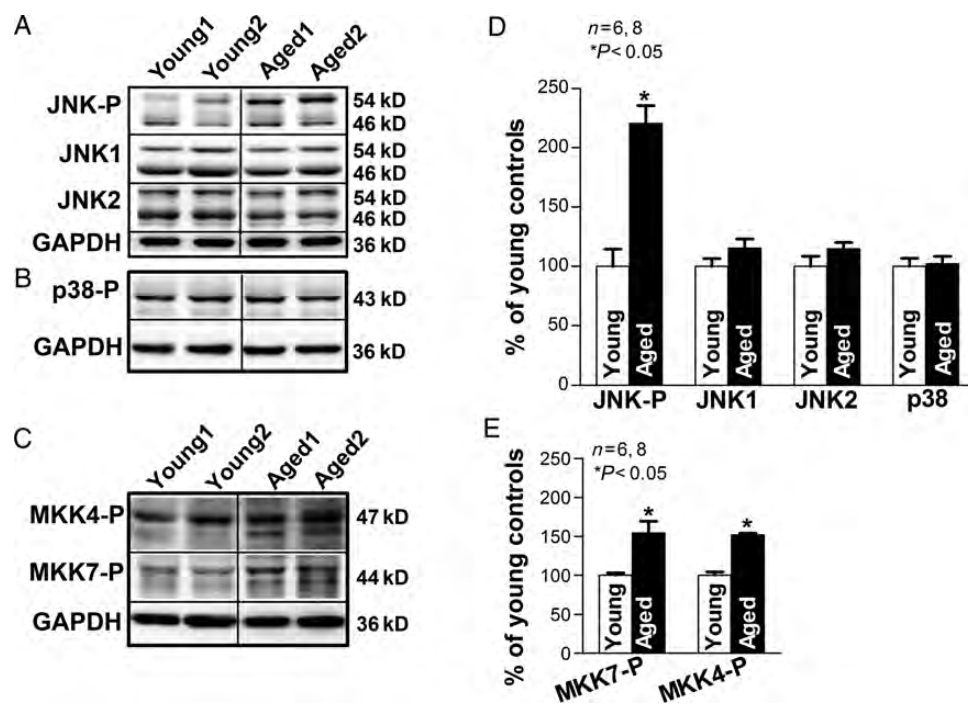


Figure 1 Enhanced JNK activation in aged rabbit LA. (A–C) Immunoblotting images of phosphorylated JNK (JNK-P), JNK1, and JNK2 (A), phosphorylated p38 (p38-P, B), and phosphorylated MKK7 and MKK4 (MKK7-P, MKK4-P; C), in young and aged rabbit LA. (D–E) Summarized data of quantified levels of JNK-P, JNK1, JNK2, p38, MKK7-P, and MKK4-P (* $P < 0.05$ vs. young).

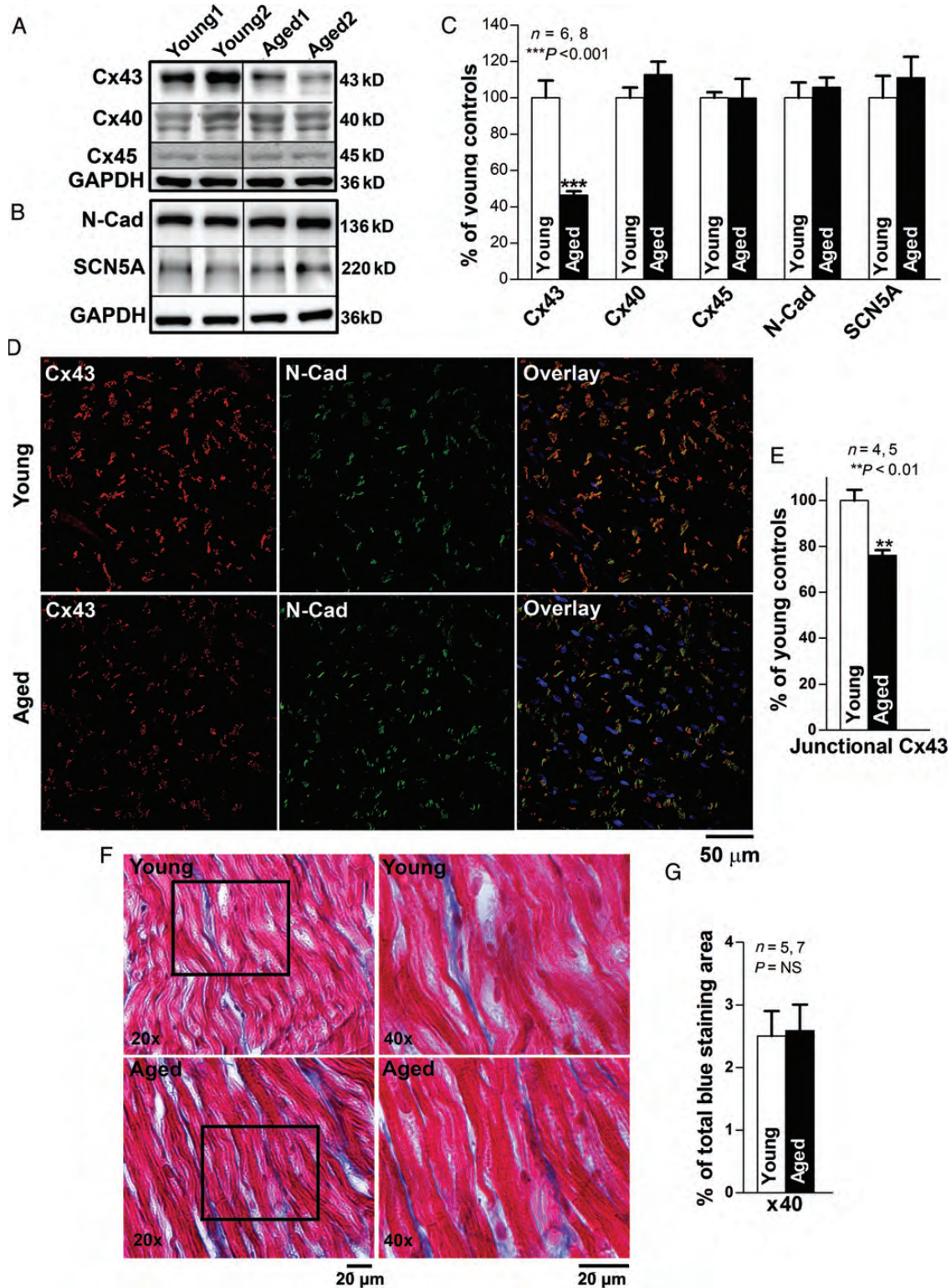


Figure 2 Marked Cx43 reduction in aged rabbit LA. (A–B) Immunoblotting images of Cx43, Cx40, Cx45, N-cadherin (N-Cad), and SCN5A. (C) Summarized data of quantified expression of Cx43, Cx40, N-Cad, and SCN5A in aged rabbit LA (** $P < 0.001$ vs. young). (D–E) Pooled data of quantified junctional Cx43 (end-to-end signals that are co-localized with N-Cad) from double immunostaining images (E) with Cx43 (green) and N-Cad (red) antibodies in aged and young rabbit LA (** $P < 0.01$). Far right column is the overlapping images of Cx43 and N-Cad (yellow) along with DAPI staining of nuclei (blue). (F) Representative images ($\times 20$ and $\times 40$) of Masson's Trichrome stained collagen (blue) and myocardium (red) in young and aged rabbit LA. Right column shows the enlarged images ($\times 40$ magnification) of the cropped areas from the left column. (G) Summarized data of quantified interstitial collagen (blue area) in aged and young rabbit LA ($P = NS$).

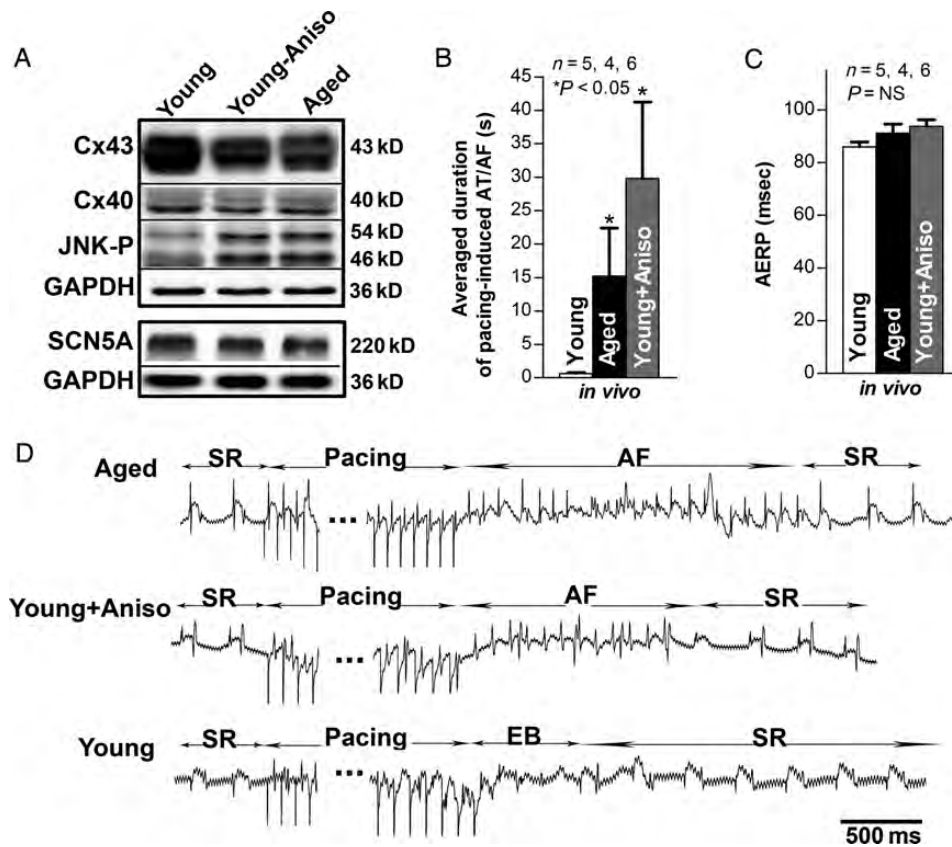


Figure 3 JNK activation is associated with Cx43 reduction and increased pacing-induced AT/AF *in vivo*. (A) Immunoblotting images of Cx43, Cx40, JNK-P, N-Cad, SCN5A in both aged rabbit LA and young rabbit LA with or without anisomycin treatment (* $P < 0.05$ and ** $P < 0.01$, respectively; $n = 4, 3, 3$). (B–C) Summarized data of average duration of pacing-induced AT/AF as well as AERP in open-chest aged rabbit LA and young rabbit LA with or without anisomycin treatment (* $P < 0.05$ and $P = \text{NS}$, respectively). (D) Representative electrograms (EG) of burst pacing (for 30 s at $\times 6$ diastolic threshold, $\text{CL} = \pm 5$ ms of atrial effective refractory period (AERP) induced AF followed by self-reversion to sinus rhythm (SR) in open-chest aged (top row) and anisomycin-challenged young rabbit LA (middle row), and self-restored SR after burst pacing induced extra beats (EB) in sham control young rabbit LA (bottom row).

AT/AF episodes per animal was 29.8 ± 11.5 s in aged, 15.2 ± 7.2 s in anisomycin-treated young rabbits, and 0.7 ± 0.1 s (duration of a few extra beats only) in untreated young controls ($P < 0.05$, ANOVA, respectively; Figure 3B and D). AERP measured at a pacing CL of 200 ms did not differ significantly between the three groups (91 ± 3 ms in aged LA, 94 ± 3 ms in anisomycin-treated young LA, and 86 ± 2 ms in untreated young LA; Figure 3C).

3.3 Increased incidence of pacing-induced arrhythmias was associated with slowed CV in aged rabbit LA *ex vivo*

To measure CV and exclude the influence of autonomic tone on AT/AF inducibility and maintenance in the aged rabbit LA, Langendorff-perfused rabbit hearts were subjected to optical mapping. Aged hearts showed a higher inducibility of pacing-induced AT/AF (8/10) than young hearts (3/9). The duration of pacing-induced AT/AF was 3.7 ± 1.4 s in aged LA vs. 0.4 ± 0.2 s (duration of a few of extra beats) in young ($P < 0.05$; Figure 4A). Aged LA showed unchanged AERP and APD_{60} vs. young controls (Figure 4B and C). These *ex vivo* data are consistent with the findings from *in vivo* studies (Figure 3).

In addition, optical mapping showed that CV was slower in aged than in young LA at the various pacing CLs ($P < 0.01$; Figure 4E and G). We found comparable values of absolute degree of heterogeneity (P_{5-95}) and heterogeneity index (P_{5-95}/P_{50}) between young and aged LA (Figure 4H). This unchanged heterogeneity of conduction is consistent with unaltered structural remodelling from our histological extracellular collagen assessment (Figure 2). The maximal upstroke slope (dV/dt_{max}) was also unaltered in aged LA vs. young controls (Figure 4D). These results indicate that slowed CV and increased arrhythmogenicity in aged rabbit LA are linked to dramatically reduced Cx43 but not structural remodelling or changes of cellular excitability.

3.4 JNK activation led to reduced Cx43, slowed CV, and increased arrhythmogenicity in cultured atrial myocytes

The specific impact of JNK activation on Cx43 suppression and arrhythmogenicity in atrial myocytes was further studied in monolayer cultures of HL-1 atrial myocytes. Treatment of HL-1 cells with 50 ng/mL anisomycin resulted in JNK activation (reflected by increased

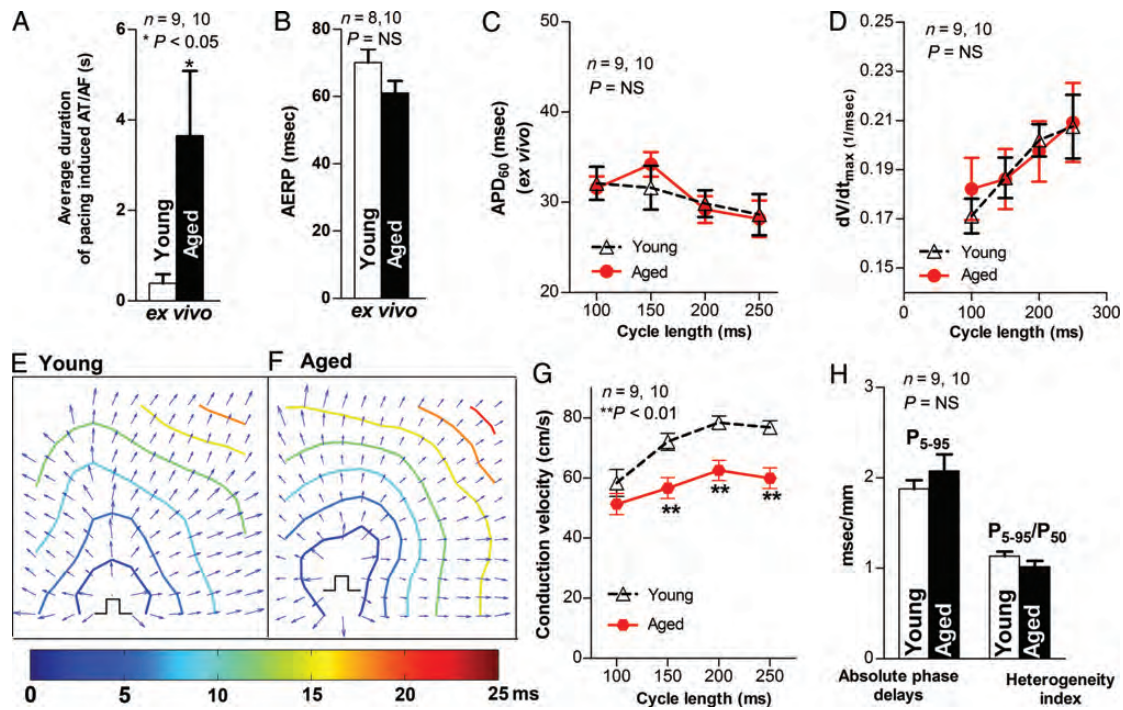


Figure 4 Increased pacing-induced AT/AF and slowed CV in aged rabbit LA *ex vivo*. (A–C) Pooled data of inducibility and duration of pacing-induced AT/AF, AERP, and APD₆₀ in Langendorff-perfused aged and young rabbit LA (**P* < 0.05, *P* = NS vs. young, respectively). (D) Summarized data for unchanged CL-dependent dV/dt_{max} in aged rabbit LA (*P* = NS). (E–F) Representative isochronal maps from young and aged rabbit hearts subjected to pacing at a CL of 200 ms (π indicates the pacing sites). (G) Summarized optical mapping CV data show that aged rabbits exhibited a CL-dependent, slower conduction (***P* < 0.01 vs. young controls). (H) Analysed optical mapping data of unchanged absolute phase delays (conduction inhomogeneity, P_{5-95}) and heterogeneity index (P_{5-95}/P_{50}) between young and aged LA (*P* = NS).

phosphorylated JNK) and reduced levels of Cx43, whereas Cx40 and SCN5A were unaffected (Figure 5A). This anisomycin-induced Cx43 suppression was consistent with the results from anisomycin-treated rabbit LA myocytes (Supplementary material online, Figure S4A and B) and neonatal rat ventricular myocytes.¹⁰ After anisomycin treatment for 16 h, five of eight monolayers exhibited rapid spontaneous rhythms (CL = 150–200 ms) that precluded pacing with 1:1 capture, whereas the remaining monolayers showed pacing-induced sustained arrhythmias (CL = 150 ms, 1 × threshold). In contrast, all sham-control monolayers (*n* = 7) had 1:1 capture in response to pacing, whereas none of the monolayers had any spontaneous activities or burst pacing-induced spontaneous activities. CV of these anisomycin-treated monolayers during spontaneous activity or pacing (CL = 200 ms; *n* = 6) was 24% slower than that in sham-controls (CL = 200 ms; *n* = 7; Figure 5C, D, and F), whereas the amount of Cx43 was reduced by 42% (*P* < 0.001, *n* = 3, 4; Supplementary material online, Figure S6A). Specific JNK inhibition by 2 μ mol/L SP600125 in 16 h anisomycin-treated monolayers (*n* = 5) prevented anisomycin-induced slowed CV and spontaneous rhythms, whereas the amount of Cx43 returned to comparable levels to that seen in sham-controls (92% of sham-controls, *n* = 3, 3; Figure 5B, E, and F, Supplementary material online, Figure S6A).

After anisomycin treatment for 24 h, all HL-1 monolayers (*n* = 7) showed irregular spontaneous rhythms (CL = 150–200 ms) that were unresponsive to electrical stimuli. CV during the spontaneous rhythm (CL = 200 ms) was slower by 41% than that of sham-controls

(Figure 5G and H), and the amount of Cx43 was further reduced by 63% after 24 h treatment with anisomycin compared with sham-controls (*P* < 0.001, *n* = 3, 3; Figure 5B and F and Supplementary material online, Figure S6A). Optical mapping also demonstrated discontinuous conduction and local conduction block in anisomycin-treated monolayers (Figure 5J and Supplementary material online, MovieS2). None of the sham-control monolayers had any spontaneous activity, and they all exhibited uniform patterns of AP propagation in response to pacing (CLs = 150 or 200 ms; *n* = 10; Figure 5I and Supplementary material online, MovieS1). With SP600125 JNK inhibition, the recovery of the Cx43 protein in the monolayers with 24 h anisomycin treatment was 76% compared with sham-controls (*n* = 3, 3; Supplementary material online, Figure S6A), but the increased Cx43 protein levels were adequate to improve conduction up to 82% of that in sham-controls (CL = 200 ms; *n* = 9, 7; Supplementary material online, Figure S6B).

To further confirm the role of JNK-induced Cx43 reduction in slowed CV and enhanced arrhythmogenicity, we infected HL-1 cells with AdCx43WT to overexpress exogenous wild-type Cx43 and with AdCx43DN to overexpress an inactive form of Cx43 after 24 h of anisomycin pre-treatment. We found that significantly increased Cx43 in AdCx43WT-infected cultures resulted in a 129% increase in CV and diminished anisomycin-induced spontaneous rhythm and discontinuous AP propagation when compared with monolayers treated with anisomycin only (*n* = 10, 7; Figure 5G, H, and K and Supplementary material online, MovieS3). In contrast, exogenous inactive Cx43DN did

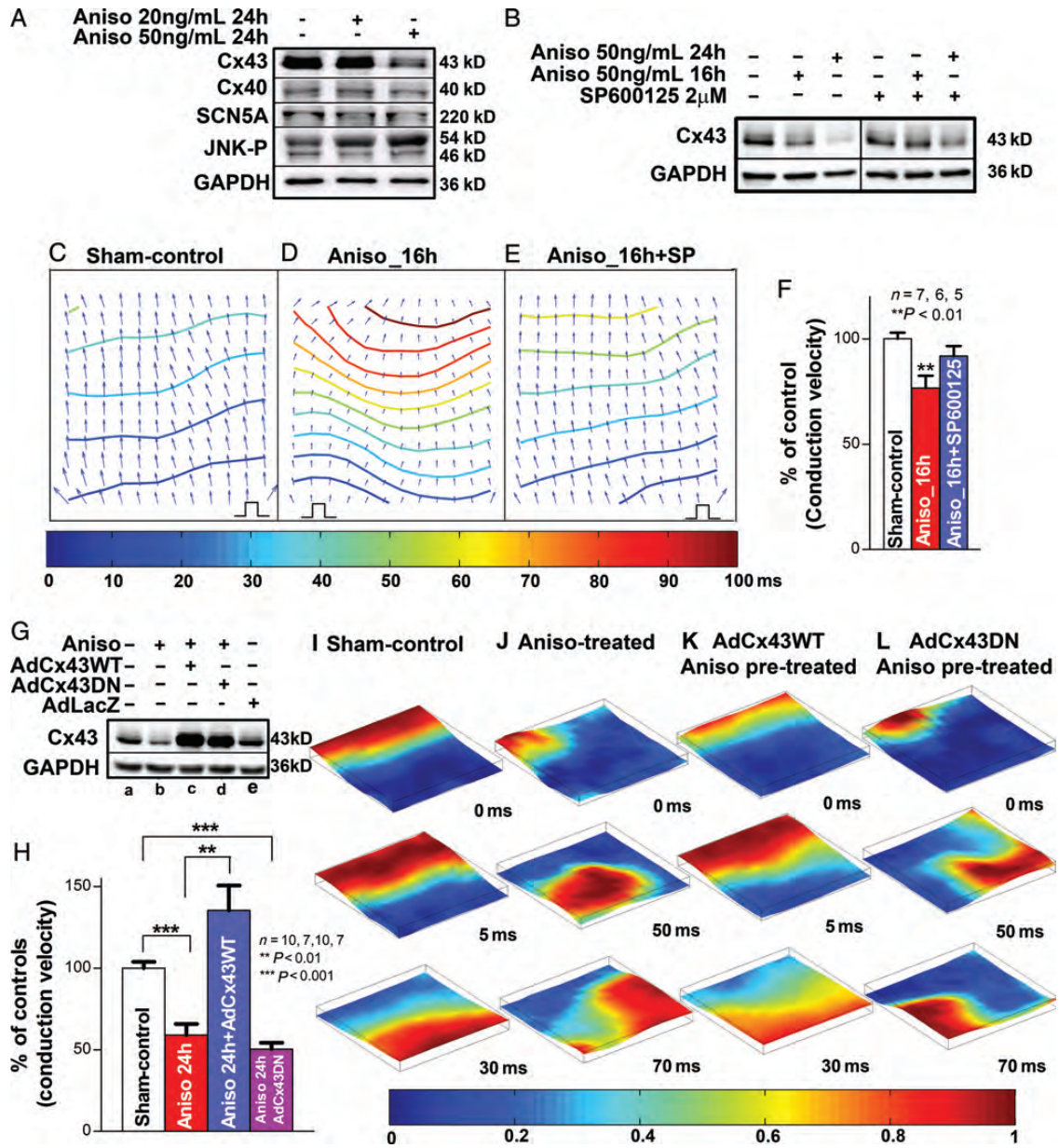


Figure 5 JNK activation contributes to Cx43 reduction and increased arrhythmogenicity in anisomycin-treated HL-1 atrial myocytes. (A) Anisomycin-induced (24 h) JNK activation is associated with a reduction in Cx43 in HL-1 atrial myocytes, whereas Cx40 and SCN5A expression were unchanged ($n = 3, 3$). (B) Immunoblotting images show progressively suppressed Cx43 after HL-1 cells treated with anisomycin for 16 h or 24 h (left panel). JNK inhibitor SP600125 blunted the effect of anisomycin-induced Cx43 reduction (right panel). (C–E) Representative isochronal maps from vehicle-treated (pacing CL = 200 ms) and anisomycin-treated (16 h, self-rhythm CL = 200 ms) HL-1 atrial monolayers with or without JNK inhibition (π indicates the self-rhythm source or the pacing sites). (F) Summarized data of CV between the three groups (** $P < 0.01$ vs. sham-control). (G) Immunoblotting images show overexpressed exogenous wild-type Cx43 (AdCx43WT, lane C) and dominant negative Cx43 (AdCx43DN-infected; lane D) in anisomycin pre-treated (24 h) HL-1 cells compared with sham-control (lane A), anisomycin-treated positive control (lane B), AdLacZ-infected negative control (lane E) ($n = 3, 3, 3, 3, 3$). (H) Summarized data of CV between sham-control, anisomycin-treated (24 h), as well as AdCx43WT-infected or AdCx43DN-infected anisomycin pre-treated monolayers (** $P < 0.01$ vs. sham-control). (I–K) Examples of uniformly propagated action potentials (CL = 200 ms) in sham-control (I) and exogenous AdCx43WT expressed anisomycin pre-treated (24 h; K) HL-1 monolayers and broken and re-entrant AP wave in an anisomycin-treated (24 h) monolayer (J) as well as in an exogenous AdCx43DN expressed anisomycin pre-treated monolayer (L). Movies of these monolayers can be found in Supplementary material online.

not reverse these JNK-induced changes ($n = 7$; Figure 5G, H, and L; Supplementary material online, Movie S4). Our results strongly suggest that JNK-induced Cx43 reduction is responsible for impaired cell coupling and enhanced arrhythmogenicity.

4. Discussion

While AF is the most common arrhythmia with a high risk of mortality and morbidity (such as due to heart failure and stroke) in the

elderly,^{4,19} pharmacological treatment and prevention strategies remain ineffective. Activation of JNK is critical for the development of cardiovascular diseases, which are associated with a dramatically increased incidence of AF.^{1,3,4} Although JNK inhibition as an anti-cancer and anti-arthritis therapy has been brought into clinical trials, contributions of JNK to AF substrate formation and development are largely unknown. Here, we report for the first time that aged rabbit LA exhibited significantly enhanced JNK signalling that was associated with significantly reduced Cx43 and increased atrial arrhythmogenicity. The direct aetiological role of JNK activation was supported by our observations that the treatment of young rabbits with the JNK activator anisomycin led to increases of activated JNK, reductions of Cx43, and increases of pacing-induced AT/AF similar to those found in aged LA. Although anisomycin may not be a specific JNK activator, studies by Petrich et al.¹⁰ showed a rescue effect with SP600125, a specific JNK inhibitor, on Cx43 expression in anisomycin-treated neonatal rat ventricular myocytes. Using cultured HL-1 atrial monolayers, we further demonstrated the pivotal role of JNK activation on Cx43 suppression and arrhythmogenicity evident from the restored amount of Cx43 and prevention of slowed CV and arrhythmogenicity by SP600125 specific JNK inhibition.¹¹ Our results strongly suggest an important role of JNK activation in the development of AF.

The abundance and distribution of connexins influences intercellular electrical coupling. Atrial gap junction channels contain predominantly Cx40, Cx43, and a lesser amount of Cx45.²⁰ In the present study, we found that JNK activation suppressed specifically Cx43 but did not affect Cx40 or Cx45 in both rabbit LA and HL-1 atrial myocytes. Previous studies have supported a major role of Cx43 in atrial conduction while the significance of Cx40 for CV and AF development remains controversial.²¹ Results from human atria⁶ and synthesized cultured strands of neonatal atrial myocytes from Cx43KO mice²² have shown that reduced Cx43 decreases CV. A recent report²¹ using a Cx43^{g60s} mutant (dominant negative) mouse model showed that a 60% reduction in atrial Cx43 along with unchanged Cx40 was linked to increased inducibility and maintainability of AF *in vivo*. Moreover, Cx43 gene transfer prevented AF development in a swine model with persistent AF.²³ Here, we demonstrated that the JNK-induced Cx43 reduction directly contributed to slowed CV and increased atrial arrhythmogenicity, because these effects were completely rescued by overexpression of exogenous wild-type Cx43 (while overexpression of inactive Cx43 had no such reversal effect). Therefore, we believe that JNK-induced Cx43 suppression is critical in AF development. It is known that JNK regulates downstream gene expression through active or inactive transcriptional factors (including c-Jun, c-fos, and SP1, which modulate Cx43 gene expression).²⁴ In addition to JNK-induced Cx43 gene down-regulation, Cx43 protein degradation could also contribute to Cx43 reduction in aged LA. Investigations are clearly needed to further understand the mechanism of JNK-regulated Cx43 suppression in aged atria.

In addition to gap junctional coupling, cardiac conduction is also determined by the active membrane properties of each cell (largely a function of Na channels) and the interstitial structural arrangement. Our results suggest that JNK activation had little impact on these factors. We observed unaltered levels of the sodium channel protein, SCN5A, and unchanged dV/dt_{max} of the APs in aged rabbit LA. Bourgeois et al.²⁵ have shown concordance of dV/dt_{max} between fluorescent signals from optical mapping recording and the electrical signals from glass microelectrode recording. Therefore, we measured dV/dt_{max} from optically mapped fluorescent signals and

found unchanged sodium channel driving AP propagation in aged intact rabbit LA. Our result is also consistent with the findings by Baba et al.²⁶ of unaltered Na channel activity from direct Na current measurement in aged canine LA myocytes. Fibrosis could impact cell–cell communication by creating barriers of dense and disorganized collagen fibrils within the interstitial space between adjacent myocytes.²⁷ However, we observed no change in interstitial fibrosis and no evidence of patchy fibrosis in aged rabbit LA, consistent with recently reported results from aged human atria.¹⁸ Moreover, our optical mapping data showed no changes in conduction heterogeneity, which also suggests the absence of structural remodelling in aged rabbit LA. Convincingly, this JNK-induced Cx43 suppression and enhanced arrhythmogenicity in aged rabbit LA was further supported by the results from anisomycin-treated young rabbit LA and cultured HL-1 atrial cells where there was no interference of interstitial fibrosis and/or changes in membrane excitability.

The pathophysiological states for AF are known to be varied and complicated in humans. When co-existing pathological conditions (such as HF, myocardial infarction) are present,⁴ co-existing cardiovascular diseases (which frequently occurs in aged human hearts) may intrinsically complicate the studies of AF development in age-dependent arrhythmogenic substrate. Our use of aged rabbits for the studies takes advantage of their many common biological features with humans,¹² but with rarely occurring cardiovascular diseases.²⁸ This allows us to exclude co-existing CVD to study age-related substrate remodelling in AF development. The aged rabbits we used in the studies compare to ~70 years in human age. These aged rabbits showed preserved cardiac function and unchanged LA size from 2D echocardiography and ECG measurements. Also, the LA tissue exhibited significantly increased ageing markers (P15^{INK}, P19^{ARF}, Supplementary material online, Figure S1A and B) reflecting valid ageing status of these rabbits. We note results in our experimental focus on the LA demonstrate an important difference in interstitial fibrosis from previous findings with the more commonly studied right atria.²⁹ Chamber differences between left and right atrium in arrhythmogenic substrate remodelling in aged hearts could be responsible for the different results in age-related atrial structural remodelling reported in the current studies and by others,^{29,30} further studies are required to elucidate this possibility.

5. Conclusions and potential implications of the results

This study demonstrates that JNK activation leads to reductions of Cx43, which impairs cell–cell communication between atrial myocytes and ultimately prompts the development of atrial arrhythmias. Activation of JNK has been shown to be critical for the development of cardiovascular diseases that are associated with a high prevalence of AF in the elderly.^{1–4} Our results shed important light on manipulation of JNK signalling (inhibition of its activation) as a novel and promising therapeutic approach to prevent and treat AF.

Acknowledgements

We graciously thank Weiwei Zhao, Sharon Melnick, and Dennis Rollins for their excellent technical assistance, Drs Li Li and Jack Rogers for their helpful advice for creating the optical mapping conduction velocity analysis program, and Kate Sreenan for her assistance in the preparation of the manuscript.

Conflict of interest: none declared.

Funding

This research was supported by American Heart Association (10GRNT3770030 to X.A.) and National Institutes of Health (HL113640 to X.A., HL067748 to V.G.F., and HL59199 to E.C.B.).

Supplementary material

Supplementary material is available at *Cardiovascular Research* online.

References

- Rose BA, Force T, Wang Y. Mitogen-activated protein kinase signaling in the heart: angels versus demons in a heart-breaking tale. *Physiol Rev* 2010;**90**:1507–1546.
- Petrich BG, Eloff BC, Lerner DL, Kovacs A, Saffitz JE, Rosenbaum DS et al. Targeted activation of c-jun n-terminal kinase in vivo induces restrictive cardiomyopathy and conduction defects. *J Biol Chem* 2004;**279**:15330–15338.
- Karin M. Inflammation-activated protein kinases as targets for drug development. *Proc Am Thorac Soc* 2005;**2**:386–390; discussion 394–385.
- Rich MW. Epidemiology of atrial fibrillation. *J Interv Card Electrophysiol* 2009;**25**:3–8.
- Saffitz JE, Davis LM, Darrow BJ, Kanter HL, Laing JG, Beyer EC. The molecular basis of anisotropy: role of gap junctions. *J Cardiovasc Electrophysiol* 1995;**6**:498–510.
- Kanagaratnam P, Rothery S, Patel P, Severs NJ, Peters NS. Relative expression of immunolocalized connexins 40 and 43 correlates with human atrial conduction properties. *J Am Coll Cardiol* 2002;**39**:116–123.
- Duffy HS, Wit AL. Is there a role for remodeled connexins in AF? No simple answers. *J Mol Cell Cardiol* 2008;**44**:4–13.
- Garner AP, Weston CR, Todd DE, Balmanno K, Cook SJ. Delta mekk3:Er* activation induces a p38 alpha/beta 2-dependent cell cycle arrest at the g2 checkpoint. *Oncogene* 2002;**21**:8089–8104.
- Hazzalin CA, Le Panse R, Cano E, Mahadevan LC. Anisomycin selectively desensitizes signalling components involved in stress kinase activation and fos and jun induction. *Mol Cell Biol* 1998;**18**:1844–1854.
- Petrich BG, Gong X, Lerner DL, Wang X, Brown JH, Saffitz JE et al. C-jun n-terminal kinase activation mediates downregulation of connexin43 in cardiomyocytes. *Circ Res* 2002;**91**:640–647.
- Bennett BL, Sasaki DT, Murray BW, O'Leary EC, Sakata ST, Xu W et al. Sp600125, an anthranyrazolone inhibitor of jun n-terminal kinase. *Proc Natl Acad Sci U S A* 2001;**98**:13681–13686.
- Ai X, Pogwizd SM. Connexin 43 downregulation and dephosphorylation in nonischemic heart failure is associated with enhanced colocalized protein phosphatase type 2a. *Circ Res* 2005;**96**:54–63.
- Alcendor RR, Gao S, Zhai P, Zablocki D, Holle E, Yu X et al. Sirt1 regulates aging and resistance to oxidative stress in the heart. *Circ Res* 2007;**100**:1512–1521.
- Fast VG, Sharifov OF, Cheek ER, Newton JC, Ideker RE. Intramural virtual electrodes during defibrillation shocks in left ventricular wall assessed by optical mapping of membrane potential. *Circulation* 2002;**106**:1007–1014.
- Eloff BC, Lerner DL, Yamada KA, Schuessler RB, Saffitz JE, Rosenbaum DS. High resolution optical mapping reveals conduction slowing in connexin43 deficient mice. *Cardiovasc Res* 2001;**51**:681–690.
- Lammers WJ, Schalij MJ, Kirchhof CJ, Allessie MA. Quantification of spatial inhomogeneity in conduction and initiation of reentrant atrial arrhythmias. *Am J Physiol* 1990;**259**:H1254–1263.
- Ai X, Zhao W, Pogwizd SM. Connexin43 knockdown or overexpression modulates cell coupling in control and failing rabbit left ventricular myocytes. *Cardiovasc Res* 2010;**85**:751–762.
- Platonov PG, Mitrofanova LB, Orshanskaya V, Ho SY. Structural abnormalities in atrial walls are associated with presence and persistency of atrial fibrillation but not with age. *J Am Coll Cardiol* 2011;**58**:2225–2232.
- Benjamin EJ, Levy D, Vaziri SM, D'Agostino RB, Belanger AJ, Wolf PA. Independent risk factors for atrial fibrillation in a population-based cohort. The Framingham heart study. *JAMA* 1994;**271**:840–844.
- Verheule S, van Kempen MJ, te Welscher PH, Kwak BR, Jongsma HJ. Characterization of gap junction channels in adult rabbit atrial and ventricular myocardium. *Circ Res* 1997;**80**:673–681.
- Tuomi JM, Tynl K, Jones DL. Atrial tachycardia/fibrillation in the connexin 43 g60s mutant (oculodentodigital dysplasia) mouse. *Am J Physiol Heart Circ Physiol* 2011;**300**:H1402–11.
- Beauchamp P, Yamada KA, Baertschi AJ, Green K, Kanter EM, Saffitz JE et al. Relative contributions of connexins 40 and 43 to atrial impulse propagation in synthetic strands of neonatal and fetal murine cardiomyocytes. *Circ Res* 2006;**99**:1216–1224.
- Bikou O, Thomas D, Trappe K, Lugenbiel P, Kelemen K, Koch M et al. Connexin 43 gene therapy prevents persistent atrial fibrillation in a porcine model. *Cardiovasc Res* 2011;**92**:218–225.
- Teunissen BE, Jansen AT, van Amersfoort SC, O'Brien TX, Jongsma HJ, Bierhuizen MF. Analysis of the rat connexin 43 proximal promoter in neonatal cardiomyocytes. *Gene* 2003;**322**:123–136.
- Bourgeois EB, Bachtel AD, Huang J, Walcott GP, Rogers JM. Simultaneous optical mapping of transmembrane potential and wall motion in isolated, perfused whole hearts. *J Biomed Opt* 2011;**16**:096020.
- Baba S, Dun W, Hirose M, Boyden PA. Sodium current function in adult and aged canine atrial cells. *Am J Physiol Heart Circ Physiol* 2006;**291**:H756–H761.
- Spach MS, Dolber PC. Relating extracellular potentials and their derivatives to anisotropic propagation at a microscopic level in human cardiac muscle. Evidence for electrical uncoupling of side-to-side fiber connections with increasing age. *Circ Res* 1986;**58**:356–371.
- Orlandi A, Francesconi A, Marcellini M, Ferlosio A, Spagnoli LG. Role of ageing and coronary atherosclerosis in the development of cardiac fibrosis in the rabbit. *Cardiovasc Res* 2004;**64**:544–552.
- Anyukhovskiy EP, Sosunov EA, Plotnikov A, Gainullin RZ, Jhang JS, Marboe CC et al. Cellular electrophysiologic properties of old canine atria provide a substrate for arrhythmogenesis. *Cardiovasc Res* 2002;**54**:462–469.
- Huang C, Ding W, Li L, Zhao D. Differences in the aging-associated trends of the monophasic action potential duration and effective refractory period of the right and left atria of the rat. *Circ J* 2006;**70**:352–357.